

## In-situ stress and fracture permeability in the Long Valley Caldera

Colleen A. Barton, Mark D. Zoback & Daniel Moos  
*Department of Geophysics, Stanford University, Calif., USA*

John H. Sass  
*US Geological Survey, Flagstaff, Ariz., USA*

**ABSTRACT:** This study examined the relationship between in situ stress, fractures and fluid flow in the Long Valley Exploratory Well (LVEW) which penetrates fractured and faulted volcanic rocks of the Long Valley Caldera in the eastern Sierra Nevada. Utilizing data from detailed analyses of stress magnitude, fracture geometry and precision temperature logs (that indicate localized fluid flow) results indicate that fluid flow along potentially active faults appears to contribute substantially to the bulk hydraulic conductivity in situ.

### 1. INTRODUCTION

While fracture-enhanced permeability depends on fracture density, orientation, and most importantly, the hydraulic conductivity of the different fracture and fault planes present the relationship between fracture and fault permeability and in situ stress is poorly understood. Fractures active in the present day stress field are generally classified as either Mode I extensile fractures, oriented perpendicular to the least principal stress (e.g., Pollard and Aydin, 1988), or Mode II or III shear fractures (potentially active faults). In this study we investigate whether fracture enhanced permeability principally results from flow along Mode I fractures (as commonly assumed) or shear (Mode II or Mode III) faults, or neither. That is, flow through highly fractured crystalline and sedimentary rock can be dominated by the orientation of faults and fractures introduced during the long geologic history of the rock mass and thus bear no genetic relation to the current stress field. In this study, we used data from a borehole that penetrates fractured and faulted igneous rocks in the LVEW to investigate the relationship between in situ stress and fracture and fault permeability.

The interaction between the state of stress and fracture characteristics is determined both by the orientation, aperture and hydraulic conductivity of the individual fractures and by the magnitudes and orientations of all three principal stresses. If active faults control fluid flow, the relative magnitudes of the three stresses determine their orientation. Laboratory studies (Jones, 1975; Nelson and Handin, 1977; Krantz et al., 1979; Trimmer et al., 1980; Tsang and Witherspoon, 1981) and theoretical models (Bawden, et al., 1980; Ayatollahi et al., 1983) agree that there is a marked decrease in fracture permeability with increasing normal load. The impact of shear displacement on permeability

appears to be a function of fracture aperture and roughness (Brown and Scholz, 1985; Brown, 1987) and there is evidence that dilatancy plays the central role in fracture conductivity under shear deformation (Tchalenko, 1970; Maini, 1971; Teufel, 1981, 1987; Makurat, 1985; Makurat, et al., 1985). Thus, the current stress field governs the current fluid activity of the fault and can explain why faults may be at different times both an avenue and a barrier to fluid flow (Hooper, 1991).

### 2. STUDY SITE, STRESS REGIME AND FRACTURING

The Long Valley Exploratory Well (LVEW) is located within the resurgent dome of the Long Valley Caldera near Mammoth Lakes in east central California (Bailey, et al., 1976). The borehole was drilled more than 2 km into rhyolites and tuffs to investigate the structure and evolution of the Long Valley Caldera. Measurements carried out in the well were designed to characterize the thermal regime, lithology, stress state, hydrology, and seismic structure within the central caldera. The rocks penetrated by the LVEW were identified by cuttings, sidewall and borehole cores. In the uppermost 622 m the borehole penetrates a post-caldera rhyolite. Between 622 m and 1890 m, it penetrates Quaternary-age Bishop Tuff, which is brecciated from 1800 to 1890 m. From 1890 to 2025 m the rock is hydrothermally altered and of uncertain age and protolith. Below 2025 m the borehole enters Paleozoic age Mt. Morrison Sierran roof pendants, primarily metapelites, shales, marbles, and metaquartzites.

Borehole televiwer data were recorded over the interval 780-2079 m. Studies of the distributions of stress-induced wellbore breakouts were conducted

and reported by Moos and Zoback (1993). The relatively few wellbore breakouts encountered in the LVEW suggests that the present-day stress field within the caldera is characterized by low horizontal stresses and a NE-SW extension direction.

The observed direction of minimum compression differs from that observed outside the caldera both in the Sierra Nevada to the West and in the Basin and Range to the East (Zoback, 1989), suggesting that stresses within the caldera are controlled by local sources. The stress orientation measured in the LVEW agrees with the inversion of earthquake focal plane mechanisms (Moos and Zoback, 1993), geodetic strain (Langbein, 1989) and active normal faults cutting through the resurgent dome (Bailey, 1977). Moos and Zoback (1993) found a strike-slip/normal faulting stress regime in the vicinity of the resurgent dome with NW-SE compression and a  $\phi$  value of about 0.7 (where  $\phi = [S_2 - S_3]/[S_1 - S_3]$ ).

Fracture and fault distribution for the study drillhole was obtained using interactive data analysis methods (described in detail in Barton et al., 1991) to measure the orientation, apparent aperture and distribution of fractures. Fracture orientation data covers the intervals 778 to 2078 m. Fractures intersected within the Bishop Tuff are predominantly steeply E or W dipping, N-S striking features. A similar set of fractures is present within the Mt. Morrison, but a secondary set of gently NW-dipping, NE-striking features are also observed.

### 3. ANALYSIS APPROACH

There are many well-documented cases where fracture density correlates with hydraulic conductivity in drillholes (Brace, 1980; Zoback and Hickman, 1982; Hess, 1985; Paillet et al., 1987; Cornet, 1989; and many others). It is also common to use geophysical logs to isolate flow horizons and measure flow characteristics (Loew, et al, 1990; Tsang et al., 1990; Goldberg et al., 1990; Long et al., 1991).

In this study we used precise temperature thermal anomalies associated with fluid flow in and out of the borehole along relatively permeable fractures and faults (Cornet, 1989). While such measurements cannot be used to make precise estimates of permeability, they are quite useful in a qualitative sense for indicating which fractures and faults are effective in conducting fluids. For example, Figure 1a shows a portion of the temperature gradient profile over the interval 780 to 980 m in the LVEW. The reference line at 25°C/km indicates the average temperature gradient in this section of the hole. Adjacent to the temperature profile is a plot of the distribution of natural fractures over the same depth interval (Figure 1b). This "tadpole" plot of depth vs. fracture dip indicates dip direction by the tadpole "tail". A closer look at the interval 819 to 823 m, provided by BHTV image data (Figure 1c), shows a natural fracture cross cutting the borehole at 821

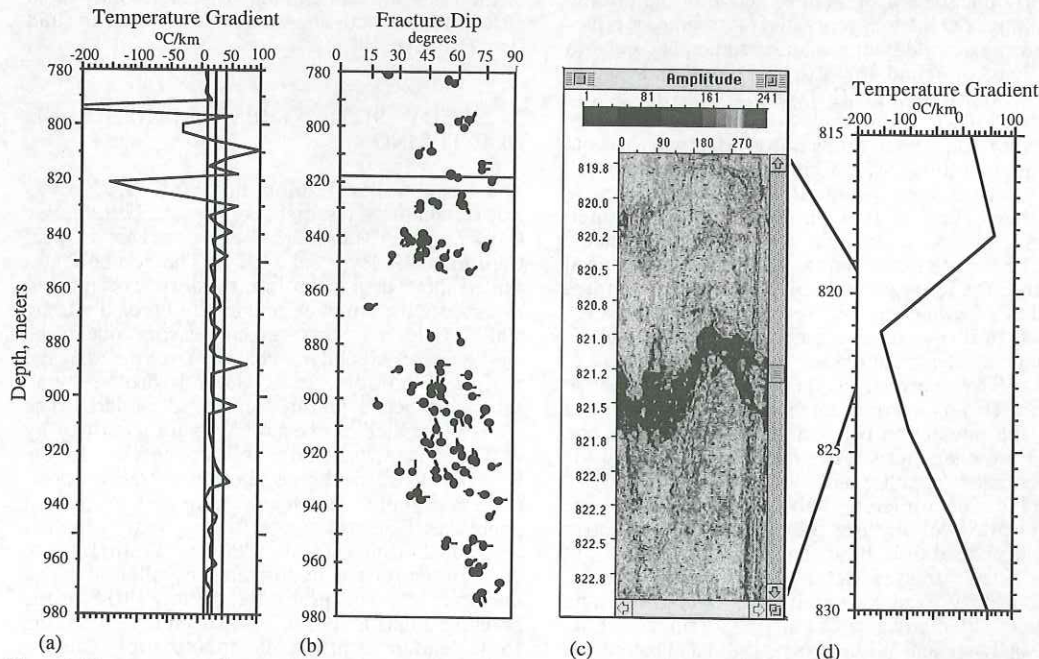


Figure 1. Temperature gradient profile (a) and analyzed fracture data (b) from the LVEW over the interval 780 to 980 m. View of BHTV data (c) near depth 821 m showing a large natural fracture corresponding to an anomaly in the temperature gradient at this depth.

m. The corresponding interval of the temperature gradient profile (Figure 1d) indicates a clear association between the depth of the fracture and that of a local temperature gradient anomaly.

To correlate the localized temperature anomalies with specific permeable fractures we isolated the obviously hydraulically conductive fractures in the LVEW based on the temperature gradient data. Temperature logs commonly contain some degree of scatter due to the extremely high sensitivity of the probe. To eliminate the exaggeration of this noise in the temperature gradient profiles a 5 point average depth smoothing was applied to the temperature data corresponding to a moving window of 1.5 m. The prominent temperature anomalies were selected by establishing a temperature gradient cutoff value above which the largest anomalies were distinct (e.g. the reference lines in Figure 1a at  $\pm 15^\circ\text{C}/\text{km}$  of the average temperature gradient).

Fractures detected with the borehole televiewer data that were within  $\pm 1.0$  m of an obvious temperature anomaly were assumed to be responsible for fluid flow at the anomaly. If more than one fracture was present within  $\pm 1.0$  m of the temperature anomaly, the dominant fracture orientation (the statistical mode) was selected. Fracture orientation was ambiguous for only 10% of the temperature anomalies. Because of the resolution limitations of the borehole televiewer, small fractures (apparent apertures less than 10 mm) that may contribute to bulk permeability may go undetected (Barton and Zoback, 1992). In this study, for example, 125 out of 135 temperature anomalies were represented by fractures detected in the image data. Thus, a relatively small number of hydraulically conductive fractures were missed by the imaging tool.

With measurements of fracture orientation and the knowledge of the orientation and magnitudes of the principal stresses in the vicinity of the fractures (from hydraulic fracturing experiments and wellbore breakout orientations) the shear,  $\tau$ , and normal,  $\sigma_n$ , stresses on each plane were computed from:

$$\tau = \beta_{11} \beta_{21} S_1 + \beta_{12} \beta_{22} S_2 + \beta_{13} \beta_{23} S_3 \quad (3.1)$$

$$\sigma_n = \beta_{11}^2 S_1 + \beta_{12}^2 S_2 + \beta_{13}^2 S_3 \quad (3.2)$$

(Jaeger and Cook, 1979) where  $\beta_{ij}$  are the direction cosines and  $S_i$  are the magnitudes of the principal stresses. The Coloumb failure criterion (assuming effective stress):

$$\tau = \mu(\sigma_n - P_p) \quad (3.3)$$

was used to indicate potentially active faults with  $0.6 \leq \mu \leq 1.0$  after Byerlee (1978). Mohr diagrams (shear versus normal stress both normalized by the vertical stress) show the population separation of fractures that are hydraulically conductive (that show

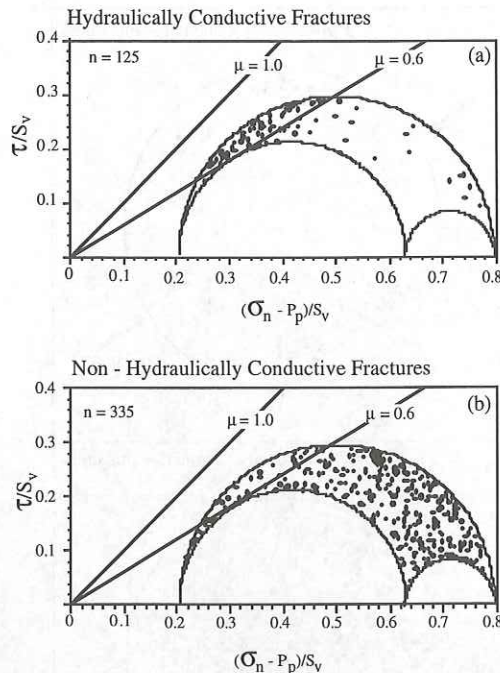


Figure 2. Mohr diagrams of fractures associated with (a) temperature anomalies and (b) fractures not associated with temperature anomalies.

significant temperature anomalies) from the non-hydraulically conductive fractures for the study drillhole (Figure 2b). As indicated by the Coloumb failure lines for  $\mu=0.6$  and  $\mu=1.0$  in Figure 2a, a large percentage of the population of temperature sensitive fractures (approximately 70%) appear to be critically stressed, potentially active faults in frictional equilibrium to the in-situ stress field. To confirm this correlation we also tested the inverse hypothesis: are fractures where there is no indication of flow *not* critically stressed? For each one meter depth interval where no temperature anomaly is detected, a fracture representing the dominant fracture trend in that interval was selected. Figure 2b shows the majority of fractures not associated with temperature anomalies. These fractures clearly lie below the Coloumb failure curve and therefore do not appear to be critically stressed Mode II and Mode III fractures.

The orientation of hydraulically conductive fractures in the LVEW represents a population distinct both from the orientation of the total fracture population and the orientation of non-hydraulically conductive fractures. Figure 3 compares lower hemisphere equal area stereonets of the population of hydraulically conductive fractures (Figure 3a) with the population of non-hydraulically conductive fractures (Figure 3b).

As mentioned above, there is abundant field,

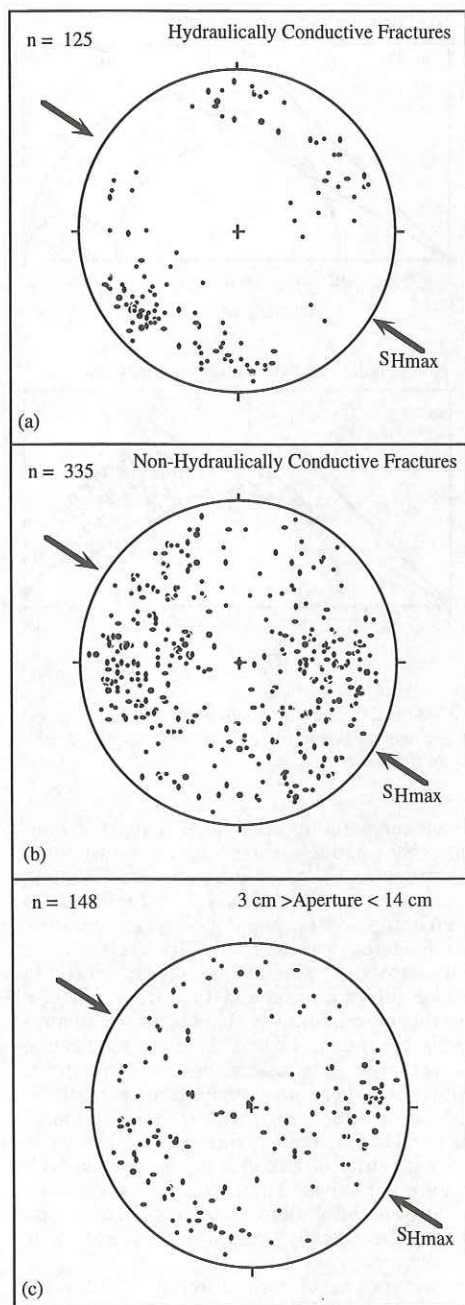


Figure 3. Equal area lower hemisphere projections of poles to (a) hydraulically conductive and (b) non-hydraulically conductive fracture planes based on precision temperature logs. (c) Poles to large aperture fractures in the LVEW.

laboratory, and theoretical evidence that shows the importance of fracture aperture to fluid flow. The use of fracture aperture to predict hydrologic flow in the crust is, however, severely limited by the lack of knowledge of which fractures actually provide open conduits for fluid flow. Geophysical logs that can be used to detect fractures include wellbore images, sonic and resistivity (Paillet et al., 1987; Cornet, 1989; Goldberg et al., 1990), however, not all methods are equally suited for delineation of a fracture's hydraulic aperture. For example, a plot of the poles to the larger apparent aperture fractures ( $> 3$  cm) measured in this study shows that fractures associated with fluid flow are not correlated with large apparent apertures. (Figure 3c). This implies that many of the large fractures in this borehole are not currently permeable pathways for fluid migration, unless these fractures are also oriented in such a way as to be potentially active, critically-stressed faults.

#### 4. SUMMARY

Borehole data from the LVEW show a significant correlation between critically-stressed fractures (that is, fractures optimally-oriented to the stress field for frictional failure) and hydraulic conductivity. This suggests that when faults are critically-stressed, permeabilities are increased and the movement of fluid along faults is possible. When faults are not optimally-oriented for failure permeabilities appear to be greatly reduced and flow is diminished. Thus, the state of stress controls many of the pre-existing planes that are likely to be hydraulically active in the LVEW. A fracture's apparent aperture as determined from wellbore image data does not necessarily bear any relationship to its potential for fluid flow.

#### ACKNOWLEDGMENTS

We thank Colin Williams of the USGS Menlo Park for providing precision temperature data for the study drillhole.

#### REFERENCES

- Ayatollahi, M. S., J. Noorishad, & P.A. Witherspoon, 1983. Stress-fluid flow analysis of fractured rock. *J. Eng. Mech.*, 109: 1-13.
- Bailey, R. A., G.B. Dalrymple, & M.A. Lanphere 1976. Volcanism, structure and geochronology of the Long Valley Caldera, Mono County, CA, *J. Geophys. Res.*, 81: 725-744.
- Barton, C. A., L. Tesler & M. D. Zoback 1991. Interactive analysis of borehole televiewer data, in *Automated Pattern Analysis in Petroleum Exploration*, edited by I. Palaz & S. Sengupta, 223-248, Springer Verlag, New York.
- Barton, C. A. & M. D. Zoback 1992. Self-similar distribution and properties of macroscopic

- fractures at depth in crystalline rock in the Cajon Pass scientific drill hole, J. Geophys. Res., 97: 5181-5200.
- Bawden, W. F., H. Curran, & J.C. Roegiers 1980. Influence of fracture deformation on secondary permeability—a numerical approach, J. Int. Rock Mech. Min. Sci. & Geomech. Abstr., 17: 265-279.
- Brace, W. F. 1978. A note on permeability changes in geologic material due to stress, Pure Appl. Geophys., 116: 627-633.
- Brace, W. F. 1980. Permeability of crystalline and argillaceous rocks, Int. J. Rock Mech. Min. Sci. & Geomech. Abstr., 17: 241-251.
- Brown, S. R. & C. H. Scholz 1985. Closure of random elastic surfaces in contact, J. Geophys. Res., 90: 5531-5545.
- Brown, S. R. 1987. Fluid flow through rock joints: The effect of surface roughness, J. Geophys. Res., 92: 1337-1347.
- Byerlee, J. 1978. Friction of rocks, Pure Appl. Geophys., 116: 615-626.
- Cornet, F. H. 1989. Survey by various logging techniques of natural fractures intersecting a borehole, Proc. of the 3rd Int. Symp. on Borehole Geophys. for Min., Geotech. & Groundwater Appl., Vol II, 559-569, Min. & Geotech. Log. Soc. of SPWLA.
- Goldberg, D., D. Speed, C. Wilkinson, E. Scholz 1990. A correlation of hydraulic conductivity from pulse tests with sonic log amplitudes, 297-302, Geological Society Special Pub.
- Hess, A. E. 1985. Identifying hydraulically-conductive fractures with a low-velocity flowmeter, Canadian Geotech. J., 23: 69-78.
- Hooper, E. C. D. 1991. Fluid migration along growth faults in compacting sediments, J. Pet. Geol., 14: 161-180.
- Jaeger, J. C. & N. G. W. Cook 1979. Fundamentals of Rock Mechanics, 3rd ed., pp., Chapman and Hall, New York.
- Jones, F. O. 1975. A laboratory study of the effects of confining pressure on fracture flow and storage capacity in carbonate rocks., J. Petrol. Tech., 27: 21-27.
- Kranz, R. L. A. D. F., T. Engelder, & C.H. Scholz 1979. The permeability of whole and jointed Barre granite, Int. J. Rock Mech. Min. Sci. & Geomech. Abstr., 16: 225-234.
- Langbein, J. 1989. Deformation of the Long Valley Caldera, Eastern California, from Mid-1983 to Mid-1988: Measurements using a two-color geodimeter, J. Geophys. Res. 94: 3833-3849.
- Long, J. C. S., K. Karasaki, A. Davey, J. Peterson, M. Landsfeld, J. Kemeny & S. Martel 1991. An inverse approach to the construction of fracture hydrology models conditioned by geophysical data., Int. J. Rock Mech. Min. Sci. & Geomech. Abstr., 28: 121-142.
- Lowe, S. Tsang, C.F., Hale, F., & P. Hufschmied 1990. The application of moment methods to the analysis of fluid electrical conductivity logs in boreholes, Report for the U.S. Dept. of Energy, LBL-28809, August.
- Maini, Y. N. T. 1971. In situ hydraulic parameters in jointed rock, their measurement and interpretation, Ph.D. Thesis, Imperial College, London, 321 p.
- Makurat, A., N. Barton & N.S. Rad 1990. Joint conductivity variation due to normal and shear deformation. in Rock Joints, Barton & Stephansson (eds), A. A. Balkema, Rotterdam, 535-540
- Makurat, A., N. 1985. The effect of shear displacement on the permeability of natural rough joints: in Hydrogeology of Rocks of Low Permeability, Newman, S.P. Chair., Memoirs, Int. Assoc. of Hydrogeologists, 17: 1: 99-106.
- Moos, D. & M.D. Zoback 1993. State of stress in the Long Valley caldera, California, Geology, 21: 837-840.
- Nelson, R. A., & J. Handin 1977. Experimental study of fracture permeability in porous rock, Amer. Assoc. Petrol. Geol. Bull., 61, 227-236.
- Paillet, F. L., A.E. Hess, C.H. Cheng, & E. Hardin 1987. Characterization of fracture permeability with high-resolution vertical flow measurements during borehole pumping, Ground Water, 25:: 28-40.
- Pollard, D. & Aydin, A. 1988. Progress in understanding jointing over the past century, Geol. Soc. Am. Bull. 100: 1181-1204.
- Tchalenko, J. S. 1970. Similarities between shear zones of different magnitudes, Geol. Soc. Am. Bull., 81: 1625-1640.
- Teufel, L. W. 1981. Pore volume changes during frictional sliding of simulated faults, in Carter, N.L. Friedman, M. Logan, J.M. & Stearns, D.W. (eds), Mechanical Behavior of Crustal Rocks, Am. Geophys. Union Mono. 24 - The Handin Volume, 135-145.
- Teufel, L. W. 1987. Permeability changes during shear deformation of fractured rock, in Proceedings 28th US Symposium on Rock Mechanics, Tucson, 473-480.
- Trimmer, D., D. Bonner, C.H. Heard, & A. Duba, 1980. Effect of pressure and stress on water transport in intact and fractured gabbro and granite, J. Geophys. Res., 85: 7059-7071.
- Tsang, C. F., P. Hufschmied, & F.V. Hale 1990. Determination of fracture inflow parameters with a borehole fluid conductivity logging method, Water Resources Res., 26: 561-578.
- Tsang, Y. W., & P.A. Witherspoon 1981. Hydromechanical behavior of a deformable rock fracture subject to normal stress, J. Geophys. Res., 86: 9287-9298.
- Zoback, M. D. & S. Hickman 1982. In situ study of the physical mechanisms controlling induced seismicity at Monticello reservoir, South Carolina, J. Geophys. Res., 87: 6959-6974.
- Zoback, M. L. 1989. The state of stress and modern deformation of the northern basin and range province. J. Geophys. Res., 94: 7105-7128.